



OPEN Flagellin recognition triggers zinc mobilization in *Arabidopsis thaliana* as a response to *Salmonella Typhimurium* invasion

Tulasi Abhinya Mandava^{1,2}, Emma Michetti¹, Maria Luisa Astolfi³, Lorenzo Camoni¹, Andrea Battistoni¹, Sabina Visconti¹✉ & Serena Ammendola¹✉

Salmonella enterica serovar Typhimurium can enter and colonize the apoplast of plants, including the edible ones, making them a potential reservoir for the pathogen and a route for human contamination. We previously showed that in *Arabidopsis thaliana* shoot colonization, *S. Typhimurium* takes advantage of its ability to export zinc primarily through the P_{1B}-type ATPase ZntA induced by zinc excess. Moreover, a plant line with reduced ability to translocate zinc from roots to shoots is more susceptible to *S. Typhimurium* shoot colonization. We, therefore, hypothesized that plants employ zinc intoxication as a defense strategy against invading bacteria. Here we show that, upon *S. Typhimurium* colonization, *A. thaliana* modulates the expression of zinc transporters, favoring the long-distance movement of the metal as well as lowering zinc storage into the plant vacuoles. Notably, we demonstrate that this strategy depends on the recognition of bacterial flagellin by the FLS2 receptor, a signal that triggers the PAMP-Triggered Immunity response in plants. Disrupting this interaction, either using an *S. Typhimurium* Δ fla strain or an *A. thaliana* *fls2* mutant line, reduces the *zntA* expression in shoot-colonizing bacteria. This observation is confirmed by a luminescent zinc biosensor assay, showing that the *A. thaliana fls2* does not increase bioavailable zinc in the *S. Typhimurium* colonized shoots. Moreover, gene expression analyses in the colonized *fls2* line revealed a downregulation of the root-to-shoot zinc translocation compared to Col-0. Overall, our results suggest that flagellin recognition by plants triggers zinc fluxes towards the invading bacteria as a facet of the PAMP-Triggered Immunity response, highlighting the importance of plant zinc homeostasis for the interaction with human pathogens.

Keywords *Salmonella*-plant interaction, PTI response, Nutritional immunity, Zinc availability, Plant zinc homeostasis

Salmonella enterica serovar Typhimurium (STM) is a major cause of human foodborne illness, frequently transmitted through raw vegetables contaminated during pre- and post-harvest procedures¹. In addition to colonizing plant surfaces, STM is able to enter plant tissues through stomata, roots, and lesions, subsequently invading the apoplast and translocating to different parts of the plant through the xylem². STM colonization of internal tissues has been reported in different edible plants, including lettuce, cilantro, tomato, and spinach, highlighting the importance of elucidating the molecular mechanisms underlying the STM-plant interaction³⁻⁶.

Plants detect invading bacteria through membrane-bound Pattern Recognition Receptors (PRRs), which recognize conserved Pathogen-Associated Molecular Patterns (PAMPs). This recognition initiates intracellular signaling cascades that activate the first layer of the plant immune system, known as PAMP-Triggered Immunity (PTI)⁷. The PTI response includes the closure of the stomata and deposition of callose to restrict pathogen invasion, and the production of reactive oxygen species and antimicrobial compounds to hamper their replication⁷. A well-studied example of bacterial PAMP is the flg22 peptide, a sequence at the N-terminus of the bacterial flagellin, highly conserved among different bacteria. In many plant species, bacterial flagellin is recognized by the Flagellin-sensitive 2 receptor (FLS2), a receptor-like kinase that initiates a phosphorylation

¹Department of Biology, Tor Vergata University of Rome, Via della Ricerca Scientifica, Rome 00133, Italy. ²PhD Program in Evolutionary Biology and Ecology, Tor Vergata University of Rome, Rome, Italy. ³Department of Chemistry, Sapienza University of Rome, P.le Aldo Moro 5, Rome 00185, Italy. ✉email: visconti@uniroma2.it; serena.ammendola@uniroma2.it

cascade, ultimately leading to transcriptional reprogramming in the plant cell⁸. Intriguingly, STM effectors delivered into plant cells interfere with host defense mechanisms, subverting them and allowing the bacteria to proliferate in the apoplast⁹.

Using the model plant *Arabidopsis thaliana*, we have demonstrated that STM colonizing the shoots expresses the Zn/Cd detoxification system *ZntA*, a P_{1B}-type ATPase that actively extrudes zinc (Zn) when its intracellular concentration exceeds the nanomolar range¹⁰. An STM *zntA* mutant is more sensitive to Zn, in vitro, and is less able to persist in *A. thaliana* shoots, unless the plant has an impaired root-to-shoot Zn mobilization^{11,12}.

Zn is one of the most essential micronutrients for plants, acting as a cofactor of more than 300 enzymes and as a structural component for many proteins, including a large number of transcription factors¹³. Zn deficiency in plants produces severe symptoms such as chlorosis, stunted growth, delayed flowering and fruiting, and weaker root systems¹³. At the same time, Zn may exert toxic effects by interacting with functional groups of proteins or by replacing other cations at their binding sites, leading to protein inactivation¹⁴. Since the range of concentrations between deficiency and toxicity is extremely narrow, the regulation of absorption, transport, and distribution of Zn, both at the tissue and cellular levels, is critical for maintaining metal homeostasis and ensuring proper plant function^{15,16}. This is accomplished by a coordinated network of membrane-bound transporters that function at different levels of uptake, translocation, and intracellular compartmentalization¹⁷. The majority of known Zn transporters belong to three main families: ZIP (zinc-regulated transporter (ZRT)/iron-regulated transporter (IRT)-like proteins)¹⁸, HMA (Heavy Metal ATPases)¹⁹, and CDF (Cation Diffusion Facilitators), also known as MTPs (Metal Tolerance Proteins)²⁰.

ZIP transporters are involved in the transport of Zn from the apoplast or organelle lumen into the cytoplasm²¹. They are particularly expressed in the root epidermis and cortex and are involved in the uptake from the rhizosphere. Most ZIP transporters appear to function redundantly to facilitate Zn influx into the root symplast^{22,23}. MTP and HMA proteins mediate the transport of cations either out of the symplast or into specific intracellular compartments. MTP1 and MTP3 are localized to the tonoplast and mediate the Zn accumulation into the vacuole to prevent cytosolic Zn toxicity^{24,25}.

In contrast, MTP2 mediates Zn transport into the endoplasmic reticulum, possibly facilitating the symplastic radial movement toward the xylem²⁶. Zn loading into the xylem is primarily driven by the P1B-type ATPases HMA2 and HMA4, which are expressed in the vascular tissues where they function redundantly to drive Zn translocation from roots to shoots¹⁹. Interestingly, HMA2 and HMA4 are essential for conferring resistance to *A. thaliana* against the necrotrophic fungus *Plectosphaerella cucumerina*²⁷.

In this study, we demonstrate that *A. thaliana* actively mobilizes Zn in response to STM colonization. Furthermore, our findings indicate that the Zn mobilization depends on the interaction between bacterial flagellin and the FLS2 receptor, suggesting that a localized modulation of Zn levels may function as a component of the defense strategy against bacterial invasion.

Results

A. thaliana mobilizes Zn towards *S. Typhimurium* colonized shoots

We have previously shown that STM exploits its Zn detoxification systems to successfully colonize *A. thaliana* shoots¹¹. However, it remained unclear whether the excess Zn sensed by STM was due to an increase in plant Zn content following colonization, as already shown for fungal invasion²⁷. To address this issue, we measured Zn content by ICP-MS in mock-treated and STM-colonized shoots, as well as in whole Col-0 seedlings (Fig. 1). As expected, we found a higher amount of Zn in the whole seedlings compared to the shoots, consistent with

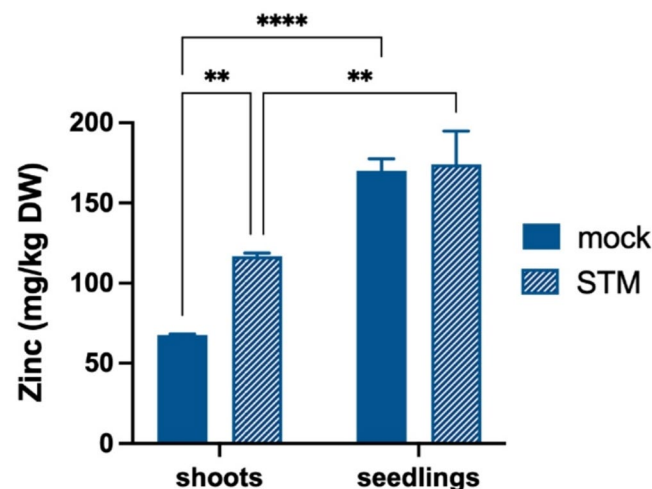


Fig. 1. Zn content in *A. thaliana* Col-0 shoots and whole seedlings. Total Zn content was measured by ICP-MS in shoots or entire seedlings at 3 days post-inoculation with STM or control buffer (mock) and normalized to the dry weight of each sample. Statistical differences were assayed by Two-way ANOVA and Tukey's multiple comparison test (** $p < 0.005$; **** $p < 0.0001$).

the role of root vacuoles as major Zn storage sites¹⁷. While no significant difference in Zn content was observed between mock and colonized whole seedlings, STM-colonized shoots exhibited a significant increase in Zn levels compared to mock-treated shoots. This may suggest that the plant responds to STM invasion by moving the Zn toward the colonized shoots rather than enhancing Zn uptake from the growth medium.

Previous studies have shown that the Zn²⁺-ATPases AtHMA2 and AtHMA4 play a role in Zn mobilization toward the site of fungal infection²⁷. Moreover, we found that in the absence of functional AtHMA2 and AtHMA4, the STM detoxification system is not critical for bacterial survival in the shoots¹¹. We, therefore, analyzed the expression of the genes encoding these Zn²⁺-ATPases, along with AtZIP5 and AtMTP2, also involved in Zn mobilization to the shoots, after inoculation of Col-0 shoots with STM. Our analysis also included transporters induced by Zn excess and involved in Zn translocation into the vacuole (i.e., AtMTP1, AtMTP3, AtHMA3) and the Golgi (AtZNE1). As shown in Fig. 2A and B, shortly after STM inoculation, Col-0 increases the transcription of genes for root-to-shoot Zn mobilization. Conversely, a general downregulation of all the genes responsible for intracellular Zn compartmentalization was observed. At a later time point (Fig. 2C and D), as STM colonization is established, Zn mobilization to the shoots remains sustained and even intensifies. Accordingly, as the Zn concentration in the shoots increases, transcription of some of the transporters involved in the movement of the metal from the cytosol to the vacuole (AtMTP1) or the Golgi apparatus (AtZNE1) is increased.

ZnT1 is necessary for shoot colonization upon flagellin recognition by FLS2

To test whether Zn mobilization is part of the PTI response to STM, we investigated the role of the flagellin-FLS2 interaction. Specifically, we used the STM Δ fla mutant that lacks flagella and the *A. thaliana* *fls2* mutant, which is unable to detect flagellin via the FLS2 receptor. First, we confirmed that the loss of flagella has no impact on the ability of STM to tolerate excess Zn in vitro (Figure S1). Moreover, the absence of flagella does not impair the

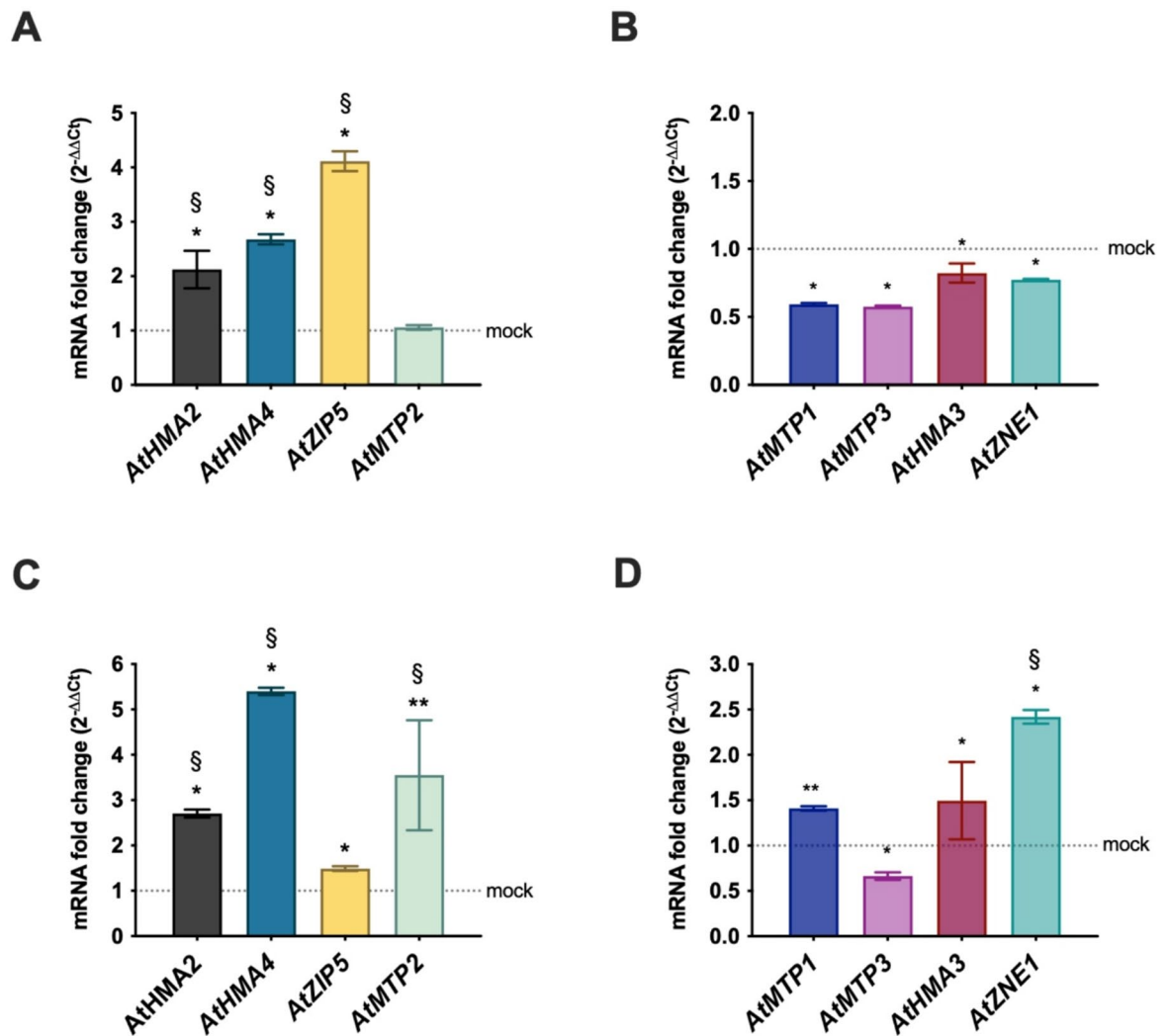


Fig. 2. Expression of Zn transporters in *A. thaliana* Col-0 following STM inoculation. Fold changes of mRNA levels were assayed by qRT-PCR at 3 h (A and B) and 3 days (C and D) after STM inoculation. Statistically significant differences between each bar and the gene expression in the mock plants (dotted lines) were assayed by the Mann-Whitney test (* $p > 0.05$; ** $p > 0.005$), $n = 3$. Fold Changes with $0.5 > FC > 1.5$ are indicated by §.

ability of STM to colonize *A. thaliana* shoots (Fig. 3A). Accordingly, the STM wild-type can similarly colonize the *fls2* mutant line, lacking the FLS2 receptor (Fig. 3B), indicating that a failure in recognizing this PAMP does not hinder STM entry or persistence in the shoots.

Next, we examined whether the absence of flagellin-FLS2 signaling affects plant Zn mobilization. We analyzed *zntA* induction in two models where the flagellin-FLS2 interaction is disrupted: (i) comparing STM wild-type and STM Δ *fla* in Col-0 plants (Fig. 4A), and (ii) comparing STM wild-type colonizing Col-0 versus *fls2* plants (Fig. 4B). In both cases, *zntA* expression is significantly reduced when the flagellin-FLS2 interaction is absent. This suggests that Zn mobilization is a flagellin-triggered PTI response sensed by STM.

To determine the relevance of the STM Zn detoxification system in this plant response, we performed competition assays between STM *zntA* mutant and STM wild-type strains in Col-0 and *fls2* shoots (Fig. 4C). As previously demonstrated, the STM wild-type outcompeted the STM *zntA* mutant in Col-0 shoots¹¹. In contrast, in *fls2* plants, competition indices were more variable and showed no significant difference between strains, consistent with reduced Zn mobilization. Together, these findings strongly indicate that STM does not sense toxic Zn concentrations in the absence of the flagellin-FLS2 interaction.

Flagellin-FLS2 interaction is necessary for Zn mobilization toward colonized shoots

Based on the observation that *zntA* induction was impaired in the absence of FLS2-mediated flagellin recognition, we hypothesized that Zn accumulation in colonized shoots may be differently regulated in the *fls2* mutant. Therefore, we measured total Zn content in shoots of mock plants or inoculated with STM using ICP-MS, comparing Col-0 and *fls2* lines. As shown in Fig. 5A, STM colonization triggers a significant increase in Zn content in Col-0 shoots, whereas Zn levels in *fls2* remain unchanged. Notably, *fls2* plants exhibit a higher

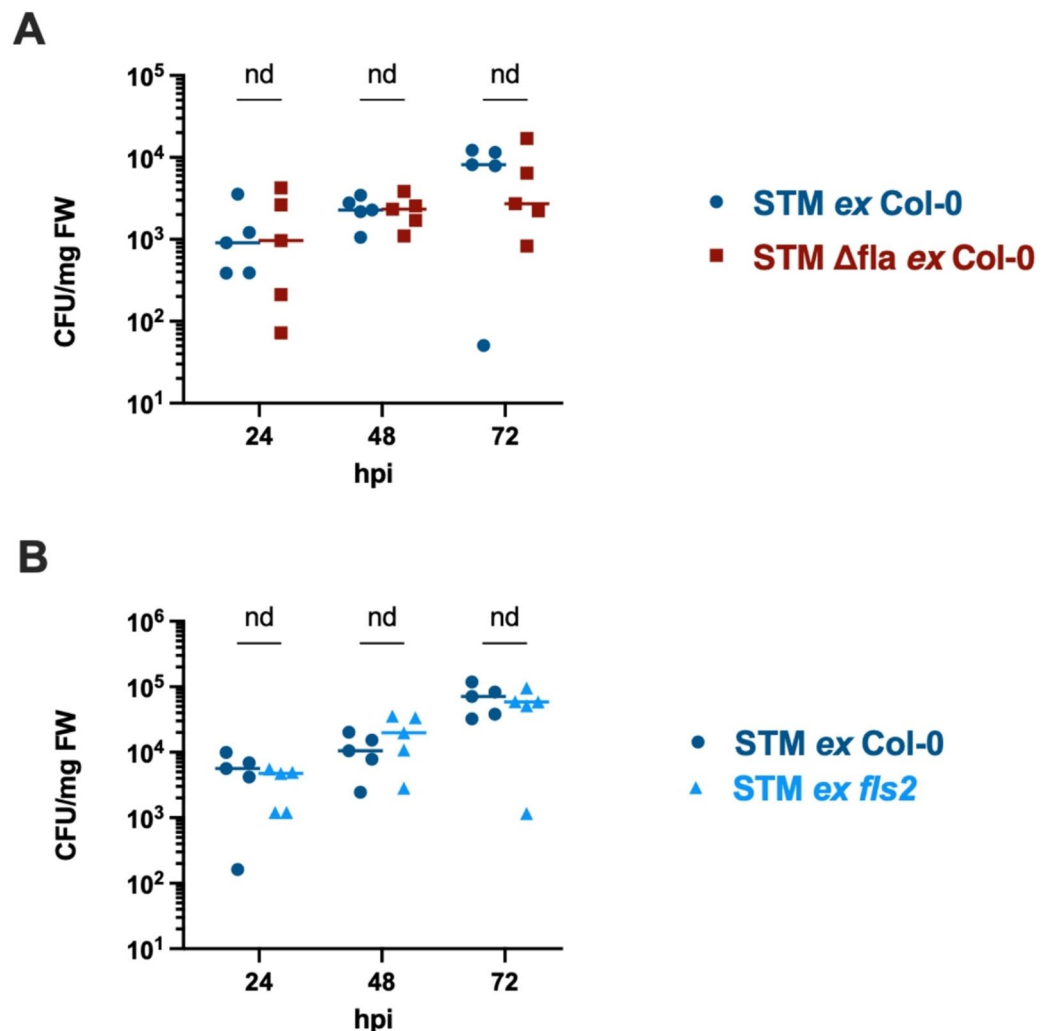


Fig. 3. Effect of flagellin-FLS2 impairment on colonization of *A. thaliana* shoots (A) Colonization of Col-0 (*ex* Col-0) by STM and STM Δ *fla*. (B) Colonization of Col-0 (*ex* Col-0) and *fls2* mutant (*ex fls2*) by STM. Bacterial loads were evaluated 24, 48, and 72 h post-inoculation (hpi). Each dot represents the CFUs/mg of fresh weight (FW) from one shoot. No statistical differences (nd) between samples at the same time point were detected (Shapiro-Wilk and Multiple unpaired t-tests).

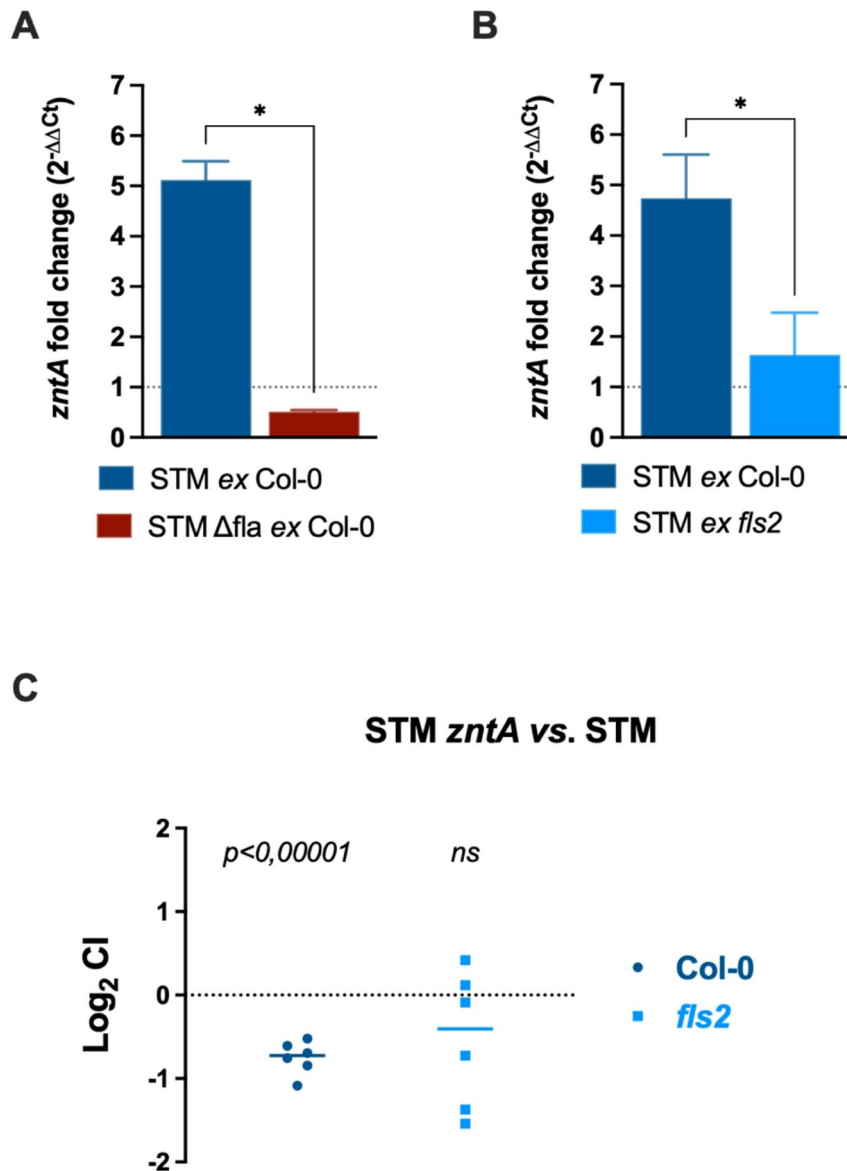


Fig. 4. Expression and impact of *zntA* in STM colonizing *A. thaliana* shoots. **(A)** qRT-PCR analysis of *zntA* induction in STM wild-type (STM) and STM lacking flagellin (STM Δ fla) recovered from Col-0 (*ex* Col-0) at 3 dpi. **(B)** qRT-PCR analysis of *zntA* induction in STM wild-type recovered from Col-0 (*ex* Col-0) or *fls2* (*ex fls2*) at 3 dpi. The horizontal dotted lines indicate *zntA* expression level in STM grown in LB medium. Statistical significance was assayed by the Mann-Whitney test ($*p > 0.05$), $n = 3$. **(C)** Competition assay in Col-0 and *fls2* shoots at 3 days post-inoculation with STM *zntA* (strain A) and STM wild-type (strain B). Each dot represents the Competitive index from one shoot, and the horizontal lines are the median values. The statistical significance of the median CI (output ratio compared to input ratio) was calculated using the Student's t-test (*ns*, not significant), after verifying the normal distribution of the datasets by the Shapiro-Wilk test.

basal Zn content than Col-0 under mock conditions. Given the low *zntA* expression previously observed in STM recovered from *fls2* plants (Fig. 4B), we hypothesized that the elevated Zn in *fls2* shoots may not be bioavailable or may be compartmentalized in a way that prevents STM from perceiving it as toxic. To verify this hypothesis, we used a luminescent bacterial biosensor, which is highly sensitive to variations of Zn availability (Figure S2). The results, reported in Fig. 5B, indicate that the basal amount of available Zn is comparable in both *A. thaliana* lines, increasing during STM colonization in the Col-0 but not in the *fls2* mutant.

To further investigate this aspect, we compared the expression of Zn transporters, whose expression was altered after STM inoculation, in the presence or absence of the flagellin-FLS2 interaction. The genes encoding the transporters involved in root-to-shoot Zn translocation are downregulated in *fls2* compared to Col-0 (Fig. 6A), suggesting that FLS2 signalling influences systemic Zn mobilization. In contrast, *AtZNE1*, involved in intracellular Zn compartmentalization, shows no significant changes between the two plant lines, indicating that Zn mobilization toward STM likely occurs through long-distance transport rather than internal redistribution

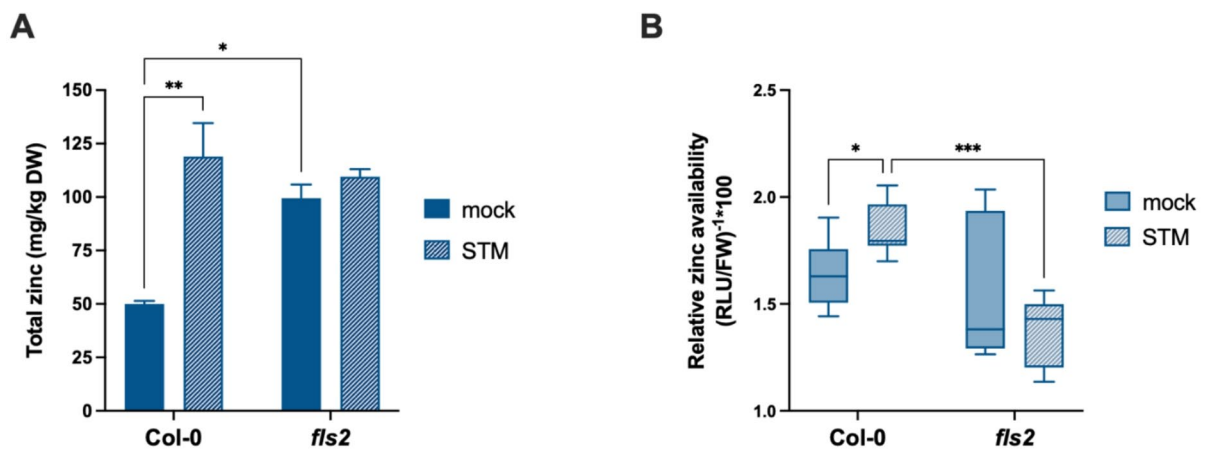


Fig. 5. Zn content in *A. thaliana* Col-0 and *fls2* shoots. **(A)** Total Zn content measured by ICP-MS in shoots inoculated or not with STM wild-type (3 dpi). Each bar represents the mean value of three pools of approximately 10 shoots each. **(B)** Relative Zn availability in Col-0 and *fls2* mock or colonized with STM (3 dpi). The groups of values represented in the boxes are calculated by the formula $[(RLU/FW)^{-1} \times 100]$, ($n=9$). Statistical differences were assayed by Two-way ANOVA and Sidak's multiple comparison tests ($*p < 0.05$; $**p < 0.005$; $***p < 0.0005$).

from cellular compartments. Accordingly, a similar expression profile can be observed in Col-0, comparing the STM wild-type with the STM Dfla colonization (Fig. 6B). Consistently, the long-distance Zn transporters are downregulated in this analysis, except for AtMTP2, which shows no significant change in expression.

Discussion

Metal intoxication was originally identified as a component of the innate immune defense in mammalian phagocytes, where it functions to kill intracellular bacteria²⁸. Upon activation by LPS or INF γ , macrophages upregulate metal transporters that accumulate metals such as Cu and Zn inside the phagolysosome²⁸. Interestingly, unicellular eukaryotes like the free-living amoeba *Dictyostelium discoideum* also employ metal intoxication as an antibacterial strategy by upregulating metal transporters homologous to those in higher eukaryotes, suggesting that this defense mechanism is evolutionarily conserved²⁹. The use of metal intoxication to fight invading microorganisms has also been suggested for plants. *Arabidopsis hallerii* and other hyperaccumulators are thought to exploit their extreme tolerance toward high metal concentration against herbivores and plant pathogens, through the so-called “elemental defense hypothesis”³⁰. Recent evidence shows that metal accumulation is associated with fungal invasion in non-hyperaccumulator plants, too. *A. thaliana* increases Zn concentration in the apoplast during *P. cucumerina* infections, as a consequence of the induction of the AtHMA2 and AtHMA4 transporters²⁷. Colonization of wheat by the powdery mildew *Blumeria graminis* is associated with ferric iron accumulation in the cell wall that promotes oxidative damage against the pathogen³⁰. Moreover, our previous research demonstrated that invading STM must express the ZntA Zn detoxification system to efficiently colonize the shoots of *A. thaliana*. Accordingly, ZntA is no longer essential when the plant accumulates less Zn in the shoots due to an impairment of the root-to-shoot Zn transport¹¹.

In this study, we demonstrate that *A. thaliana* responds to STM colonization by actively redistributing Zn toward the site of bacterial invasion (Figs. 1 and 2). This response is related to the induction of key long-distance Zn transporters, including AtHMA2, AtHMA4, and AtMTP2. An additional and less characterized transporter from the ZIP family, AtZIP5, is also upregulated during the early stages of colonization. Interestingly, a homolog of ZIP5 was recently reported to be upregulated in tomato plants in response to STM infection, suggesting a conserved role across species³¹. The increased Zn accumulation likely supports the activity of Zn-dependent enzymes and Zn-finger transcription factors involved in the plant response to invading bacteria. However, the increase in *zntA* expression clearly suggests that the metal is, at least in part, perceived by the invading bacteria and sensed as toxic¹¹. Moreover, at early time points after STM colonization, we observe a slight but still significant downregulation of *AtMTP1* and *AtMTP3*, which are involved in Zn sequestration from the cytosol into the vacuole (Fig. 2B). This may allow a rapid Zn mobilization to the apoplast, which is the compartment where STM resides⁹. Interestingly, it has been demonstrated that *AtMTP3* silencing increases Zn content in the shoots, suggesting that this transporter plays a role in restricting the Zn root-to-shoot movement²⁴. Zn mobilization toward the site of the invasion is maintained over time (Fig. 2C), while the host plant buffers the increased Zn flux as suggested by the significant induction of the Golgi-localized transporter AtZNE1, and a slight increase in the transcription of *AtMTP1* (Fig. 2D)³². Accordingly, at later time points, *AtZIP5* is no longer induced. ZIP transporters are positively regulated by the transcription factors bZIP19 and bZIP23, which are inactivated by Zn binding when the metal is highly available in the cytosol^{33,34}.

We hypothesized that the Zn redistribution is a targeted response to microbial recognition by the plant, triggered by the perception of STM flagellin by FLS2. The role of flagella in STM colonization of plants is still controversial and depends on the experimental model analyzed^{35,36}. However, a recent study has shown that both

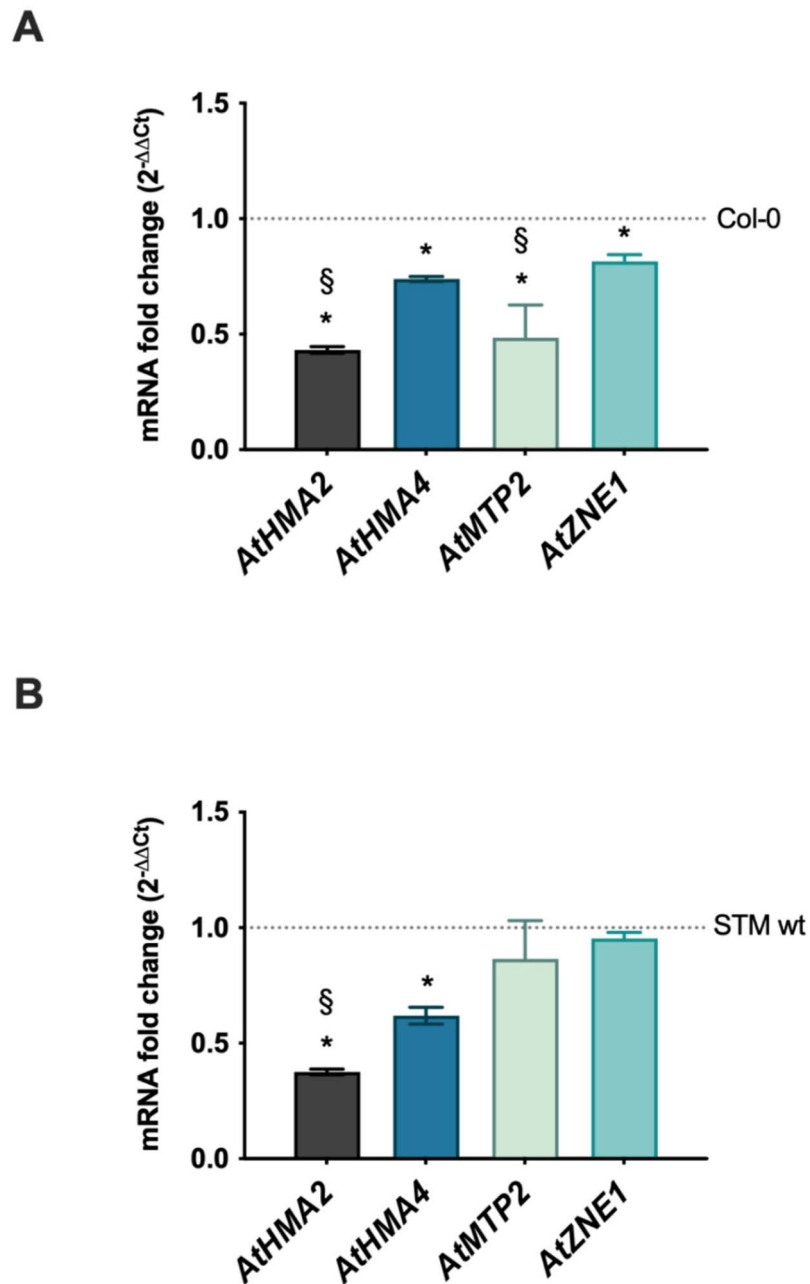


Fig. 6. Impaired flagellin-FLS2 interaction affects the expression of *A. thaliana* Zn transporters. **(A)** Fold changes of transcription were assayed by qRT-PCR in *fls2* compared to Col-0 (dotted line) at 3 days post-inoculation with STM wild-type. **(B)** Fold changes of transcription were assayed by qRT-PCR in Col-0 at 3 days post-inoculation with STM Dfla compared with Col-0 colonized by STM wild-type (dotted line). Statistically significant differences were assayed by the Mann-Whitney test ($*p > 0.05$), $n = 3$. Fold changes with $0.5 > FC > 1.5$ are indicated by §.

colonization and persistence of STM in tomato plants do not require the presence of flagella and that flagellin expression becomes heterogeneous in the STM population during long-term colonization³⁷. In our model, STM colonization and persistence in *A. thaliana* shoots are not affected by the presence of flagellin or FLS2 (Fig. 3), unlike plant pathogens as *P. syringae* that can be advantaged by the absence of the FLS2 receptor³⁸. However, disruption of the flagellin-FLS2 interaction leads to a significant downregulation of *zntA* in STM colonizing the plants (Fig. 4A and B). This indicates that, in the absence of the PTI activation, the bacteria do not experience Zn toxicity. The competition assay further strengthens our hypothesis: in *fls2* plants, STM *zntA* mutant is not outcompeted by STM wild-type, supporting the functional relevance of the flagellin-FLS2 interaction for the Zn mobilization following STM invasion (Fig. 4C). Indeed, the measurement of the shoot Zn content indicates that there is no increase in the colonized *fls2* shoots, compared to the mock-treated samples (Fig. 5A). However, we noticed that basal Zn content in the *fls2* mutant is significantly higher than that in the Col-0 line. This was

unexpected, since no previous evidence correlates the FLS2 receptor to Zn homeostasis in the absence of a flagellin stimulus. A more comprehensive analysis of differentially regulated genes in the *fls2* mutant compared to Col-0 may help clarify whether the absence of the FLS2 receptor influences pathways involved in Zn uptake or storage, potentially revealing a role for FLS2 beyond PAMP recognition.

The observation of the higher Zn content in the *fls2* mutant compared to the Col-0 shoots appeared in striking contrast with the low *zntA* expression in STM colonizing the *fls2* mutant (Fig. 4B). However, using a whole-cell biosensor, we demonstrate that the amount of free Zn is similar in the two plant lines, and it increases only in Col-0 following STM colonization (Fig. 5B). This reporter strain was previously employed to investigate Zn availability in a *Galleria mellonella* model, demonstrating that invertebrate hosts employ nutritional immunity mechanisms relying on Zn deprivation to control pathogen growth³⁹. The lower amount of free Zn in the *fls2* colonized shoots compared to Col-0 agrees with the observation that expression of Zn transporters is downregulated in the absence of flagellin-FLS2 interaction (Fig. 6). The increase of Zn perceived by STM likely occurs in Col-0 apoplast, where these bacteria reside, and where the metal is weakly buffered by the cell wall polysaccharides rather than sequestered by proteins¹³.

In conclusion, our results indicate that the recognition of flagellin by FLS2 initiates a shift in Zn distribution, specifically directing Zn fluxes toward the site of bacterial invasion, and contributing to plant defense via localized metal stress. Concomitantly, we observed a decrease in Zn transport toward compartments not accessible to the apoplast-localized bacteria. This targeted mobilization of Zn appears to be an integral component of the PTI response, since it is abrogated in the absence of flagellin-FLS2 interaction. Although the downstream signaling events connecting flagellin perception to Zn transporter activation remain to be fully elucidated, it is plausible that canonical PTI components are involved. For instance, receptor-associated kinases such as BIK1, MAP kinase cascades (MPK3/6), and WRKY transcription factors have well-established roles in transcriptional reprogramming during immune responses and could similarly regulate genes encoding Zn transporters⁷. Further work is needed to test these hypotheses and to dissect how PTI integrates micronutrient homeostasis into immune signaling networks, along with a precise evaluation of subcellular Zn localization. Moreover, it would be valuable to investigate whether this response can be triggered by PAMPs other than bacterial flagellin and to extend this analysis to edible plants that can act as a reservoir of enteric human pathogens. Although plants are not typically considered conventional hosts for STM, the ability of these enterobacteria to colonize leafy vegetables, cereals, and fruits poses a significant threat to human health¹. Also, expanding the analysis to additional plant-pathogen systems will allow us to generalize this response mechanism and strengthen the concept of a plant nutritional immunity, or elemental defense hypothesis, where the host manipulates micronutrient availability to inhibit pathogens, either by withholding or by overloading⁴⁰. The discovery that *A. thaliana* activates a defense response involving Zn mobilization through a PAMP-mediated mechanism provides a foundation for future studies aimed at developing innovative strategies to mitigate the risks associated with the consumption of contaminated plant-derived foods. This study highlights the critical role of adequate Zn supplementation in agriculture for enhancing plant resistance to pathogenic microorganisms, while simultaneously improving the nutritional quality of crops.

Materials and methods

Reagents

All the chemicals required for the solutions were bought as ultrapure reagents from Sigma-Aldrich (Sigma-Aldrich Corporation, St. Louis, MO). ZnSO₄ was freshly dissolved in ultrapure water as a 0.5 M solution, suitably diluted, and used within a few days. The antibiotics were dissolved as 1000X concentrated stock solutions, then sterilized using filtration and stored at -20 °C.

Bacterial strains and growth conditions

The bacterial strains and plasmids used in this study are listed in Table S1. Bacteria were streaked from glycerol stocks on Luria Bertani Agar plates (LBA) or *Pseudomonas* Isolation Agar (PIA) supplemented with antibiotic when needed (for *E. coli* and STM, 10 µg/mL gentamicin and 50 µg/mL kanamycin; for *P. aeruginosa*, 100 µg/mL gentamicin) and routinely grown in Luria Bertani medium (LB) at 37 °C with aeration. Vogel-Bonner Minimal Medium (VBMM: 0.192 g/L MgSO₄ · 7H₂O, 2 g/L citric acid, 10 g/L anhydrous K₂HPO₄, 3.5 g/L NaNH₄HPO₄ · 4H₂O, 2 g/L glucose, 2 µM FeSO₄) was used for *P. aeruginosa* growth under Zn-limiting conditions, as already described⁴¹.

Plant lines and growth conditions

The *Arabidopsis thaliana* wild-type line ecotype Columbia-0 (Col-0) was derived from a laboratory collection. The *fls-2* mutant line (SALK_141277), lacking the FLAGELLIN SENSING 2 receptor FLS2, was obtained from the Nottingham Arabidopsis Stock Center. The seedlings were grown in half-strength MS (2.2 g/L) (Duchefa Biochemie), 0.05% MES (Sigma-Aldrich), pH 5.7. In the end, 0.8% agar was added to the medium, and then it was sterilized for 20 min at 121 °C by autoclaving and poured into Petri dishes to solidify. *A. thaliana* seeds were sterilized in 70% ethanol for 1 min and then in 3% sodium hypochlorite, 0.05% Tween-20 for 10 min, mixing by vortex once every 2 min. The seeds were washed four times with sterile water under a laminar flow hood, sown on MS along a single line (14–16 seeds per plate), and left in the dark at 4 °C to stratify for three days. Plates were placed vertically in a growth chamber at 22 °C, and a photoperiod of 16/8 hours light/dark.

Salmonella typhimurium colonization of Arabidopsis Thaliana

Single colonies of the bacterial strains were inoculated in LB broth and grown at 37 °C with aeration overnight. The cultures were then diluted 1:100 in fresh LB broth and grown at 37 °C for 2 h until an OD₆₀₀ of 0.4–0.6. The bacterial suspension was then diluted to 10⁷ CFU/ml in 0.5 mM Potassium Phosphate buffer and used

to colonize 10-day-old *A. thaliana* shoots, as previously described¹¹. Briefly, the shoot of each seedling was wet with 0.05 ml of the bacterial suspension, withdrawing the excess liquid from the plate shortly after. The plants were harvested and utilized at varying time intervals, according to the experiment. For bacterial count, each *A. thaliana* shoot was placed in 1.5 ml microcentrifuge tubes, weighed on an analytical balance (model BP121S Sartorius), and surface-sterilized for 2 min using a sterilizing solution (phosphate-buffered saline (PBS) containing 0.1% SDS, 0.2% Tween 20, and 1% NaClO), then extensively washed with sterile ddH₂O. After adding 0.2 ml of 0.01 M MgCl₂ and 20% glycerol, the shoots were mechanically homogenized using a sterile micro pestle. The homogenates were diluted in PBS and plated on LBA. For bacterial enumeration, the number of colonies from each homogenate was related to the weight of the shoot and reported as CFU/mg of fresh weight (FW).

RNA extraction and qRT-PCR analysis

Total RNA was extracted from *A. thaliana* Col-0 and *fls2* seedlings colonized or not colonized (hereafter referred to as mock) with STM. For each experimental condition, groups of 20–25 plants were pooled, frozen with liquid nitrogen, and mechanically ground to a fine powder using a mortar and pestle (previously treated with chloroform to inactivate RNases and cooled). RNA was extracted from 100 mg of powdered plant tissue using the RNeasy Plant Mini Kit RNA (Qiagen) and stored at –80 °C. Bacterial RNA from LB cultures of STM was obtained from mid-log phase grown inocula (OD₆₀₀ = 0.5–0.6). An aliquot corresponding to approximately 10⁷ cells was employed for RNA extraction using the RNeasy mini kit (Qiagen GmbH) according to the manufacturer's instructions. The concentration and purity of the RNA from plant homogenates and bacterial cultures were determined with a NanoDrop™ Lite Spectrophotometer (Thermo Fisher Scientific).

RNA extracted from plant homogenates and bacteria grown in LB was used for cDNA synthesis by retrotranscribing 1 µg of RNA using PrimeScript™ Reagent Kit (Takara Bio Inc.) according to the manufacturer's instructions.

The primers used for qRT-PCR analyses are listed in Table S2. The reactions were performed in triplicate using SYBR GREEN dye (PCR Biosystems) and the QuantStudio3 apparatus (Applied Biosystems), with the following parameters: (i) initial denaturation at 95 °C for 2 min; (ii) 45 cycles of denaturation at 95 °C for 10 s, primer annealing at 58 °C for 20 s and extension at 65 °C for 20 s; (iii) melting curve, from 55 °C for 1 min. The mRNA fold induction was calculated using the ΔΔCt method⁴² using *UBIQUITIN10* for *A. thaliana* and *gmk* for STM as housekeeping genes.

Competition assay

Bacterial competition assays in *A. thaliana* seedlings were performed as previously described¹¹. Briefly, STM *zntA* mutant (strain A) and STM wild-type (strain B) were streaked on LBA plates, and a single colony of each strain was inoculated into the LB medium. The cultures were grown at 37 °C with aeration until reaching an OD₆₀₀ of approximately 0.5–0.6. Subsequently, the bacterial suspensions were diluted to 10⁷ CFU/mL and mixed in a 1:1 ratio in 0.5 mM potassium phosphate buffer, pH 7.4. A suitable dilution of the mixture was plated on LBA and replica-plated on LBA supplemented with kanamycin, to determine the input ratio. The bacterial mixture was used to colonize *A. thaliana* shoots. At 3 days post-inoculation, the shoots were homogenized, and suitable dilutions of the homogenates were plated on LBA. The next day, the plates were replica-plated on LBA supplemented with kanamycin to evaluate the output ratios. The competitive index (CI) was calculated for each shoot, as the ratio of the output to the input of strain A to strain B, using the formula:

$$CI = (Output\ STMzntA / STM\ wt) / (Input\ STMzntA / STM\ wt)$$

Statistical significance was determined by comparing the input and output ratios using the Student's t-test.

Salmonella Typhimurium zinc sensitivity assay

Overnight LB cultures of STM wild-type, STM Dfla, and STM *zntAzitB* mutant were normalized to an OD₆₀₀ of 0.1, corresponding to approximately 10⁸ CFU/ml. Serial tenfold dilutions were prepared in a sterile PBS buffer to achieve a range of concentrations from 10¹ to 10⁶, then 5 µl of each dilution was spotted onto LBA plain or supplemented with 0.5 mM ZnSO₄. The plates were incubated at 37 °C for 16–18 h for the evaluation of growth inhibition.

ICP-MS analysis

The total Zn content in plants was determined in colonized and mock plants by an inductively coupled plasma mass spectrometer (ICP-MS, model 820-MS; Bruker), as already described¹¹. For sample preparation, the shoots of 10-day-old infected seedlings were weighed and washed with 1 mM EDTA to remove divalent cations, which eventually contaminates the surface of the plants, and then washed 4 times with ddH₂O. The shoots or the entire seedlings were dried at 60 °C for 48 h. Subsequently, the samples were accurately weighed (dry weight, DW) using an analytical balance and prepared for ICP-MS analysis of Zn content. The total Zn content was reported as mg/kg dry weight (DW).

Zinc bioavailability assay

Ten-day-old seedlings of *A. thaliana* Col-0 and *fls2* mutant were either mock-treated or colonized by STM. At 3 days post-inoculation, the fresh weight of shoots was recorded, and tissues were carefully homogenized to minimize external Zn contamination. Homogenates were centrifuged, and the supernatants were collected.

The *PzrmA*-lux biosensor was generated by tri-parental mating, in which the *PzrmA*-lux plasmid was mobilized from *E. coli* DH5α donor cells into *Pseudomonas aeruginosa* PA14, using *E. coli* HB101 harboring

pRK2013 as the helper strain, as previously described³⁹. Exconjugants were selected on PIA supplemented with gentamicin. The biosensor strain was pre-cultured in LB medium and then diluted 1:1000 in VBMM, where it was grown overnight to induce Zn limitation. The overnight culture was subsequently diluted to 5×10^7 CFU/mL in fresh VBMM for use in the assay.

For each measurement, 180 μ L of the biosensor suspension was dispensed into black-walled, clear-bottom 96-well microplates and incubated for 10 min with 20 μ L of plant-derived supernatant, in technical triplicate. As controls, the biosensor was exposed to increasing concentrations of ZnSO₄ (1 mM to 100 mM) or EDTA (6.25 mM to 25 mM) under the same conditions. Luminescence, recorded as Relative Luminescence Units (RLUs), was measured using a Sunrise™ microplate reader (Tecan) with an integration time of 1000 ms, and values were normalized to the corresponding shoot fresh weight. Relative Zn availability was calculated as $[(RLU/FW)^{-1} \times 100]$.

Statistical analyses

Multiple unpaired t tests, Mann-Whitney test, and Two-way ANOVA with multiple comparison tests were performed using the GraphPad 10 software, as specified in each figure caption. Prior to applying the t-test, we checked if the normal distribution model fits the data by the Shapiro-Wilk test, obtaining a p-value > 0.05 for every dataset.

Data availability

All data generated or analysed during this study are included in this published article and its supplementary information files.

Received: 1 August 2025; Accepted: 24 November 2025

Published online: 01 December 2025

References

- Kowalska, B. Fresh vegetables and fruit as a source of Salmonella bacteria. *Ann. Agric. Env. Med.* **30**, 9–14 (2023).
- Kroupitski, Y. et al. Internalization of Salmonella enterica in leaves is induced by light and involves chemotaxis and penetration through open stomata. *Appl. Environ. Microbiol.* **75**, 6076–6086 (2009).
- Goudeau, D. M. et al. The Salmonella transcriptome in lettuce and Cilantro soft rot reveals a niche overlap with the animal host intestine. *Appl. Environ. Microbiol.* **79**, 250–262 (2013).
- Golberg, D., Kroupitski, Y., Belausov, E., Pinto, R. & Sela, S. Salmonella typhimurium internalization is variable in leafy vegetables and fresh herbs. *Int. J. Food Microbiol.* **145**, 250–257 (2011).
- Zheng, J. et al. Colonization and internalization of Salmonella enterica in tomato plants. *Appl. Environ. Microbiol.* **79**, 2494–2502 (2013).
- Johnson, N., Litt, P. K., Kniel, K. E. & Bais, H. Evasion of plant innate defense response by Salmonella on lettuce. *Front. Microbiol.* **11**, 506502 (2020).
- DeFalco, T. A. & Zipfel, C. Molecular mechanisms of early plant pattern-triggered immune signaling. *Mol. Cell.* **81**, 3449–3467 (2021).
- Garcia, A. V. et al. Salmonella enterica Flagellin is recognized via FLS2 and activates PAMP-triggered immunity in Arabidopsis Thaliana. *Mol. Plant.* **7**, 657–674 (2014).
- Zarkani, A. A. & Schikora, A. Mechanisms adopted by Salmonella to colonize plant hosts. *Food Microbiol.* **99**, 103833 (2021).
- Wang, D., Hosteen, O. & Fierke, C. A. ZntR-mediated transcription of ZntA responds to nanomolar intracellular free zinc. *J. Inorg. Biochem.* **111**, 173–181 (2012).
- Visconti, S., Astolfi, M. L., Battistoni, A. & Ammendola, S. Impairment of the Zn/Cd detoxification systems affects the ability of Salmonella to colonize Arabidopsis Thaliana. *Front. Microbiol.* **13**, 1–12 (2022).
- Huang, K. et al. Investigation of the role of genes encoding zinc exporters zntA, zitB, and fieF during Salmonella typhimurium infection. *Front. Microbiol.* **8**, 2656 (2018).
- Broadley, M. R., White, P. J., Hammond, J. P., Zelko, I. & Lux, A. Zinc in plants. *New Phytol.* **173**, 677–702 (2007).
- Zlobin, I. E. Current Understanding of plant zinc homeostasis regulation mechanisms. *Plant. Physiol. Biochem.* **162**, 327–335 (2021).
- Zlobin, I. E., Kartashov, A. V., Nosov, A. V., Fomenkov, A. A. & Kuznetsov, V. V. The labile zinc pool in plant cells. *Funct. Plant. Biol.* **46**, 796–805 (2019).
- Lanquar, V. et al. Dynamic imaging of cytosolic zinc in Arabidopsis roots combining FRET sensors and rootchip technology. *New Phytol.* **202**, 198–208 (2014).
- Sinclair, S. A. & Krämer, U. The zinc homeostasis network of land plants. *Biochim. Biophys. Acta - Mol. Cell. Res.* **1823**, 1553–1567 (2012).
- Guerinot, M. & Lou The ZIP family of metal transporters. *Biochim. Biophys. Acta - Biomembr.* **1465**, 190–198 (2000).
- Hussain, D. et al. P-type ATPase heavy metal transporters with roles in essential zinc homeostasis in Arabidopsis. *Plant. Cell.* **16**, 1327–1339 (2004).
- Montanini, B., Blaudez, D., Jeandroz, S., Sanders, D. & Chalot, M. Phylogenetic and functional analysis of the cation diffusion facilitator (CDF) family: improved signature and prediction of substrate specificity. *BMC Genom.* **8**, 1–16 (2007).
- Eide, D. J. Zinc transporters and the cellular trafficking of zinc. *Biochim. Biophys. Acta - Mol. Cell. Res.* **1763**, 711–722 (2006).
- Lee, S. et al. Redundant roles of four ZIP family members in zinc homeostasis and seed development in Arabidopsis Thaliana. *Plant. J.* **108**, 1162–1173 (2021).
- Ochoa Tufiño, V. et al. Arabidopsis Thaliana Zn transporter genes ZIP3 and ZIP5 provide the main Zn uptake route and act redundantly to face Zn deficiency. *Plant. J.* **121**, e17251 (2025).
- Arrivault, S., Senger, T. & Krämer, U. The Arabidopsis metal tolerance protein AtMTP3 maintains metal homeostasis by mediating Zn exclusion from the shoot under Fe deficiency and Zn oversupply. *Plant. J.* **46**, 861–879 (2006).
- Desbrosses-Fonrouge, A. G. et al. Arabidopsis Thaliana MTP1 is a Zn transporter in the vacuolar membrane which mediates Zn detoxification and drives leaf Zn accumulation. *FEBS Lett.* **579**, 4165–4174 (2005).
- Sinclair, S. A. et al. Systemic upregulation of MTP2- and HMA2-Mediated Zn partitioning to the shoot supplements local Zn deficiency responses. *Plant. Cell.* **30**, 2463–2479 (2018).
- Escudero, V. et al. Arabidopsis Thaliana Zn²⁺-efflux ATPases HMA2 and HMA4 are required for resistance to the necrotrophic fungus plectosphaerella cucumerina BMM. *J. Exp. Bot.* **73**, 339–350 (2022).
- Sheldon, J. R. & Skaar, E. P. Metals as phagocyte antimicrobial effectors. *Curr. Opin. Immunol.* **60**, 1–9 (2019).

29. Hanna, N. et al. Zn²⁺ Intoxication of *Mycobacterium marinum* during dictyostelium discoideum infection is counteracted by induction of the pathogen Zn²⁺ Exporter CtpC. *MBio* **12**, 1–15 (2021).
30. Liu, G. et al. Targeted alterations in iron homeostasis underlie plant defense responses. *J. Cell. Sci.* **120**, 596–605 (2007).
31. Zarkani, A. A. et al. *Salmonella* adapts to plants and their environment during colonization of tomatoes. *FEMS Microbiol. Ecol.* **95** (11), fiz152 (2019).
32. Wang, Y., Yang, J., Miao, R., Kang, Y. & Qi, Z. A novel zinc transporter essential for Arabidopsis zinc and iron-dependent growth. *J. Plant. Physiol.* **256**, 153296 (2021).
33. Assunção, A. G. L. et al. Arabidopsis Thaliana transcription factors bZIP19 and bZIP23 regulate the adaptation to zinc deficiency. *Proc. Natl. Acad. Sci. U S A.* **107**, 10296–10301 (2010).
34. Lilay, G. H. et al. Arabidopsis bZIP19 and bZIP23 act as zinc sensors to control plant zinc status. *Nat. Plants.* **7**, 137–143 (2021).
35. Shaw, R. K. et al. Cellulose mediates attachment of *Salmonella enterica* serovar typhimurium to tomatoes. *Environ. Microbiol. Rep.* **3**, 569–573 (2011).
36. Berger, C. N. et al. Interaction of *Salmonella enterica* with Basil and other salad leaves. *ISME J.* **3**, 261–265 (2009).
37. Zarkani, A. A. et al. *Salmonella* heterogeneously expresses flagellin during colonization of plants. *Microorganisms* **8** (6), 815 (2020).
38. Zipfel, C. et al. Bacterial disease resistance in Arabidopsis through Flagellin perception. *Nature* **428**, 764–767 (2004).
39. Michetti, E. et al. Modelling host – pathogen interactions: *Galleria mellonella* as a platform to study *Pseudomonas aeruginosa* response to host-imposed zinc starvation. *Microbiology (Reading)* **171** (1), 0015241–13 (2025).
40. Hörger, A. C., Fones, H. N. & Preston, G. M. The current status of the elemental defense hypothesis in relation to pathogens. *Front. Plant Sci.* **4**, 395 (2013).
41. Mastropasqua, M. C. et al. Growth of *Pseudomonas aeruginosa* in zinc poor environments is promoted by a nicotianamine-related metallophore. *Mol. Microbiol.* **106**, 543–561 (2017).
42. Schmittgen, T. D. & Livak, K. J. Analyzing real-time PCR data by the comparative C(T) method. *Nat. Protoc.* **3**, 1101–1108 (2008).

Author contributions

T.A.M., M.L.A. and E.M. performed the experiments; S.V. and S.A. designed the experiments and wrote the manuscript; L.C. and A.B. revised the manuscript draft. All authors reviewed the manuscript.

Declarations

Competing interests

The authors declare no competing interests.

Additional information

Supplementary Information The online version contains supplementary material available at <https://doi.org/10.1038/s41598-025-30356-z>.

Correspondence and requests for materials should be addressed to S.V. or S.A.

Reprints and permissions information is available at www.nature.com/reprints.

Publisher's note Springer Nature remains neutral with regard to jurisdictional claims in published maps and institutional affiliations.

Open Access This article is licensed under a Creative Commons Attribution-NonCommercial-NoDerivatives 4.0 International License, which permits any non-commercial use, sharing, distribution and reproduction in any medium or format, as long as you give appropriate credit to the original author(s) and the source, provide a link to the Creative Commons licence, and indicate if you modified the licensed material. You do not have permission under this licence to share adapted material derived from this article or parts of it. The images or other third party material in this article are included in the article's Creative Commons licence, unless indicated otherwise in a credit line to the material. If material is not included in the article's Creative Commons licence and your intended use is not permitted by statutory regulation or exceeds the permitted use, you will need to obtain permission directly from the copyright holder. To view a copy of this licence, visit <http://creativecommons.org/licenses/by-nc-nd/4.0/>.

© The Author(s) 2025